Modelling the simple shear behaviour of clay considering principal stress rotation

Nan Lu[1], Yunming Yang[2]*, Hai-Sui Yu[3], Zhe Wang[4]

[1]Department of Civil Engineering, International Doctoral Innovation Centre, University of Nottingham Ningbo China, Ningbo 315100, PR China.
[2]Ningbo Nottingham New Materials Institute, University of Nottingham Ningbo China, Ningbo 315100, PR China
[3]School of Civil Engineering, University of Leeds, Leeds LS2 9JT, UK
[4]Department of Civil Engineering, Faculty of Engineering, Lishui University, Lishui 323000, PR China

*ming.yang@nottingham.edu.cn
Tel.: +86-18668290219 (Y. Yang)

Abstract

Simple shear deformation is prevailing in geotechnical problems. One of its salient features is the rotation of the principal stress axes. Early numerical modelling of soil simple shear behaviour usually neglects the plastic deformation induced by principal stress rotation. Recent attempts at accurately modelling the sand simple shear behaviour have accounted for this loading mechanism, but those for the clay simple shear modelling are rare. To fill the gap, this paper presents a simple constitutive model for the simulation of clay simple shear behaviour with consideration of the effect of the principal stress rotation. The model uses a non-associative flow rule and incorporates an additional mechanism associated with the principal stress rotation. The new mechanism caters for the soil non-coaxiality and plastic volumetric response under pure rotation of principal stress axes. Stress-strain incremental linearity is maintained in the proposed model. Comparisons of simulations with clay simple shear test data justify the importance of the principal stress rotation. The model satisfactorily captures the undrained shear strength. The soil non-coaxial behavior is also well reproduced.

Keywords: clay constitutive model, simple shear, principal stress rotation, undrained shear strength, non-coaxiality.

1. Introduction

The simple shear type of deformation exists in many geotechnical engineering applications. For example, soils adjacent to a friction pile or underneath an offshore foundation, deform essentially in the simple shear mode. In the laboratory, the simple shear deformation is duplicated, in general, using the direct simple shear apparatus. Criticisms against the simple shear test are mainly for two reasons: the non-uniform stress and strain distribution within the soil specimen, and the lack of lateral stress measurement in the routine simple shear tests. Despite these drawbacks, the simple shear test has apparent advantages such as the ease of setting up and rapid consolidation [1], the ability to apply some rotation of principal stress axes [2], and most importantly, the relevance to in situ conditions.

Early numerical modelling of soil simple shear behaviour was focused on the stress and strain non-uniformity and the influence of boundary conditions [3-5]. The effect of the principal stress rotation is usually neglected for simplicity. However, it has been long recognized through experiments that the principal stress directions have strong impacts on the soil strength and deformation characteristics [6-9]. Roscoe [2] reported that the principal directions of stress and plastic strain rate are non-coaxial (known as non-coaxiality) in the presence of the principal stress rotation in the simple shear. A few attempts at modelling the effect of the stress rotation in the simple shear were made recently. Osinov and Wu [10] and Yang and Yu [11] numerically evaluated the influence of the principal stress rotation on the soil stress-strain response and non-coaxiality in the simple shear. Gutierrez *et al.* [12] proposed a two-dimensional sand model which incorporates a non-coaxial stress-dilatancy relation and an anisotropic strength criterion. Jefferies *et al.* [13] idealized the influence of the principal stress rotation as the 'shrink' of the yield surface and simulated the cyclic simple shear tests of sand. Nevertheless, most of these models were dedicated to the sand modelling, whilst those for the clay simple shear behaviour are rare. Responses of sand and clay are very different and usually require different types of yield surfaces and flow rules.

Therefore, the objective of this paper is to develop a constitutive model for the clay behaviour during monotonic simple shearing with specific consideration of the principal stress rotation. The model is based on a non-associative version of the classical Modified Cam-Clay (MCC) model [14]. The effect of principal stress rotation is considered by including an additional plastic loading mechanism. The proposed model is validated by comparing the simulation results with those from the associative and non-associative MCC models (i.e., without considering the principal stress rotation), and with the clay simple shear experimental date.

2. Model formulation

By applying the additive decomposition of the total strain rate, one has

$$\dot{\varepsilon}_{ij} = \dot{\varepsilon}_{ij}^e + \dot{\varepsilon}_{ij}^p \tag{1}$$

where the superscripts e and p denote elastic and plastic components, respectively. The elastic relation is the same as that in the MCC model, which is expressed in terms of the bulk and shear moduli defined as follows

$$K = \frac{1+e}{\kappa} p \; ; \; G = \frac{3(1-2\nu)}{2(1+\nu)} K \tag{2}$$

where e is the void ratio, κ is the slope of the swelling line in the e-ln$p$ space, and ν is the Poisson's ratio. The plastic strain rate, $\dot{\varepsilon}_{ij}^p$, consists of two components. The first component, denoted by $\dot{\varepsilon}_{ij}^{pc}$, is associated with the conventional plastic loading (superscript c). The second part, denoted by $\dot{\varepsilon}_{ij}^{pr}$, is associated with the loading mechanism of principal stress rotation (superscript r). The development of $\dot{\varepsilon}_{ij}^{pc}$ and $\dot{\varepsilon}_{ij}^{pr}$ is described below.

2.1. Non-associative clay plasticity model

The proposed model uses the MCC type ellipse for the yield and plastic potential surfaces. Following Jiang *et al.* [15], the critical state stress ratio M is used to configure the plastic potential, and another parameter N is used to configure the yield surface. Thus, the plastic potential reads as

$$g = \frac{q^2}{M^2} - p(p_g - p) = 0 \tag{3}$$

and the yield surface reads as

$$f = \frac{q^2}{N^2} - p(p_0 - p) = 0 \tag{4}$$

where $p = (1/3)\sigma_{kk}$ and $q = \sqrt{(3/2)s_{ij}s_{ij}}$ with s_{ij} being the deviatoric stress tensor; p_g is the value of p at the intersection between the plastic potential surface and the p-axis, and p_0 is

the hardening parameter. As the soil is saturated in the paper, the effective stress principle is used, in which the total stress is the summation of the effective stress and excess pore pressure. The stress symbol denote the effective stress in the paper, or specified otherwise. Fig 1 gives a schematic illustration of the two surfaces in the p-q space. The figure also shows the conventional loading direction $l_{ij}^c = \partial f / \partial \sigma_{ij}$ and flow direction $R_{ij}^c = \partial g / \partial \sigma_{ij}$. The value of p_g is determined by substituting the current stress into Eqn (3), and the value of p_0 is prescribed by a hardening rule the same as that in the MCC model, reads as

$$\dot{p}_0 = \frac{(1+e)p_0}{\lambda - \kappa} \dot{\varepsilon}_{kk}^{pc} \qquad (5)$$

where λ is the slope of the normal compression line in the e-$\ln p$ space. The parameters M and N are defined to be functions of the Lode angle θ, reads as

$$M = M_c \left[\frac{2c^4}{(1+c^4) - (1-c^4)\sin 3\theta} \right]^{1/4} \qquad (6a)$$

$$N = N_c \left[\frac{2c^4}{(1+c^4) - (1-c^4)\sin 3\theta} \right]^{1/4} \qquad (6b)$$

and

$$-\frac{\pi}{6} \leq \theta = \frac{1}{3}\sin^{-1}(\frac{27}{2}\frac{J_3}{q^3}) \leq \frac{\pi}{6} \qquad (7)$$

where $c = M_e / M_c$ with M_e and M_c being the values of M at triaxial extension and compression, respectively, N_c is the value of N at triaxial compression, and $J_3 = (1/3)s_{ij}s_{jk}s_{ki}$. The plastic potential and yield surfaces are always convex provided $c \geq 0.6$ [16]. Note that the parameters M and N have the same interpolation rule (the same ratio c enters both Eqns (6a) and (6b)), indicating an associative flow rule in the π-plane. It will be shown later that such a choice simplifies the model formulation. The N is in general (but not necessarily) smaller than M. For the special case of $N=M$, the associative MCC model is retrieved. Jiang *et al.* [15] showed that the non-associative model can better capture the shear strength of clays in the triaxial test, but its performance in the simple shear hasn't been investigated.

2.2. Loading mechanism of principal stress rotation

This section deals with the additional plastic loading mechanism associated with the principal stress rotation. This mechanism is defined by

$$wl_{ij}^r \dot{\sigma}_{ij} - K_p^r L^r = 0 \qquad (8a)$$

$$w = \left\langle 1 - (\eta/M)^m \right\rangle \qquad (8b)$$

where $\eta = q/p$ is the stress ratio, and l_{ij}^r, K_p^r and L^r are the loading direction, plastic modulus and loading index in the new mechanism, respectively, and $\langle \ \rangle$ is the Macaulay bracket that prevents a value from being negative. The m is a large positive number which will render $w \approx 1$ when $\eta < M$, and $w=0$ when $\eta > M$. A default value of $m=50$ is selected in this work. The function of w is adopted to freeze this mechanism when soils yield on the 'dry' side of the yield surface. This

simplification is because the influence of pure principal stress rotation on soils with $\eta > M$ is not known up to date as no experimental investigation has been conducted under this condition. A similar concept was firstly used by Gao and Zhao [17].

It is assumed that the loading direction l_{ij}^r follows the direction of the principal stress rotation (i.e., the direction orthogonal to the current principal stress directions). For a stress vector $\sigma_{ij} = (\sigma_x, \sigma_y, \sigma_z, \sigma_{xy}, \sigma_{yz}, \sigma_{zx})$, consider the simple case where the intermediate principal stress direction is fixed at the Z-direction. In this case, the principal stress rotation takes place in the plane of $((\sigma_x - \sigma_y)/2, \sigma_{xy})$. Then, the l_{ij}^r is defined as follows

$$l_{ij}^r = (-a, \quad a, \quad 0, \quad b) \qquad (9a)$$

$$a = \frac{l_{xy}^c}{\sqrt{(l_x^c - l_y^c)^2/4 + (l_{xy}^c)^2}} \ ; \ b = \frac{(l_x^c - l_y^c)/2}{\sqrt{(l_x^c - l_y^c)^2/4 + (l_{xy}^c)^2}} \qquad (9b)$$

A schematic illustration of the definition of l_{ij}^r is shown in Fig 2. Note that Eqns (9) are not exactly the direction of the principal stress rotation because the l_{ij}^c, instead of σ_{ij}, is used to define l_{ij}^r. This selection is based on the theoretical consideration that l_{ij}^r should be orthogonal to l_{ij}^c. Nevertheless, Eqns (9) can approximate the direction of stress rotation satisfactorily. Likewise, if the principal stress rotation takes place in the planes of $((\sigma_y - \sigma_z)/2, \sigma_{yz})$ and of $((\sigma_z - \sigma_x)/2, \sigma_{zx})$, the corresponding loading directions can also be defined. Combing them altogether, a complete l_{ij}^r is obtained.

The plastic modulus, K_p^r, is proposed as

$$K_p^r = h_r \left(\frac{M^2 - \eta^2}{2\eta} \right)^{0.2} \qquad (10)$$

where h_r is a new material parameter. The power relation in Eqn (10) is to make this loading mechanism less sensitive when approaching the critical state, where the principal stress rotation is about to cease in the simple shear. It is seen from Eqn (10) that for a hydrostatic stress state ($\eta=0$), $K_p^r = \infty$, indicating the physical meaning that no rotation of principal stress axes at hydrostatic state.

To complete the mechanism, a flow rule is proposed for soils subjected to pure principal stress rotation, reads as

$$\dot{\varepsilon}_{ij}^{pr} = L^r l_{ij}^r + |L^r| \sqrt{\frac{2}{3}} D^r \delta_{ij} \qquad (11)$$

where $| \ |$ is the symbol of absolute value, D^r is the dilatancy ratio in this mechanism, and δ_{ij} is the Kronecker delta. A subtle point here is that no Macaulay bracket is used to prevent the loading index L^r from being negative. The reason behind it is because Eqns (9) implicitly assumed a direction of anticlockwise rotation in the plane of $((\sigma_x - \sigma_y)/2, \sigma_{xy})$, which can either be along or opposite to the correct direction of stress rotation. For the latter case, a negative L^r is obtained from Eqn (8a). However, it does not affect the results because

the $L^r l_{ij}^r$ in Eqn (11) always gives the correct deviatoric flow directed along, and not opposite to, the direction of principal stress rotation. Meanwhile, the absolute value symbol on the L^r in front of D^r in Eqn (11) ensures that the contraction or dilation is by all means determined by the sign of D^r. According to Eqns (11) and (9), the deviatoric plastic strain in the z-direction is always zero in this mechanism, which can be inaccurate. A remedying approach is to use $N_{ijkl}^t l_{kl}^r \big/ \left\| N_{ijkl}^t l_{kl}^r \right\|$ as the deviatoric flow direction, where $\| \ \|$ denote the norm and N_{ijkl}^t is the *deviatoric tangential projection tensor* [18]. A recent study [19] showed that in the simple shear, these two deviatoric flow rules produce almost identical results. Therefore, the simpler choice of Eqn (11) is kept. Now the last variable to be defined is the dilatancy ratio, D^r. Experimental results showed that various soils subjected to pure principal stress rotation tend to be contractive [20,21,9]. Thus, the following expression is proposed

$$D^r = d_r \frac{M^2 - \eta^2}{2\eta}[1 - \exp(-V\gamma^r)] \tag{12}$$

where d_r is a new material parameter, and γ^r is the cumulativeness of the plastic strain induced by this mechanism. The V is another large positive constant and has a default value of $V=100$ in this work. The terms in the brackets render $D^r \approx 0$ when $\gamma^r \approx 0$. They are introduced for computational stability at the initiation of simple shear loading as a strong rotation of stress may bring the updated stress point inside the yield surface and causing numerical problems.

2.3. Incremental elastoplastic relation

Since the deviatoric flow is associative for the conventional loading, and note that the l_{ij}^r is deviatoric and orthogonal to the l_{ij}^c, one obtains $l_{ij}^r R_{ij}^c = 0$. Then, using this relation in conjunction with Eqn (8a) and the conventional consistency condition $\dot{f} = 0$, the two loading indices for conventional loading and principal stress rotation can be respectively derived as

$$L^c = \frac{l_{ij}^c E_{ijkl} \dot{\varepsilon}_{kl} - \tilde{K} l_{mm}^c L^r}{K_p^c + l_{st}^c E_{stpq} R_{pq}^c}; \quad L^r = \frac{2Gw}{K_p^r + 2Gw} l_{kl}^r \dot{\varepsilon}_{kl} \tag{13}$$

and

$$\tilde{K} = sign(L^r) \sqrt{\frac{2}{3}} K D^r \tag{14}$$

where K_p^c is the plastic hardening (or softening) modulus, E_{ijkl} is the elastic stiffness tensor and $sign(L^r)$ denotes the sign of L^r. Eqn (13) shows that with the inclusion of the additional mechanism for principal stress rotation, the L^c is coupled with the L^r provided $D^r \neq 0$. Finally, using Eqns (1) and (13), the rate formed elastoplastic stress-strain relation becomes

$$\dot{\sigma}_{ij} = E_{ijkl}^{ep} \dot{\varepsilon}_{kl}$$

$$= \left[E_{ijkl} - \frac{E_{ijab} R_{ab}^c l_{cd}^c E_{cdkl}}{K_p^c + l_{st}^c E_{stpq} R_{pq}^c} \right] \dot{\varepsilon}_{kl} \tag{15}$$

$$- \frac{2Gw}{K_p^r + 2Gw} \left[(2G l_{ij}^r + \tilde{K} \delta_{ij}) l_{kl}^r - \frac{\tilde{K} l_{mm}^c E_{ijab} R_{ab}^c l_{kl}^r}{K_p^c + l_{st}^c E_{stpq} R_{pq}^c} \right] \dot{\varepsilon}_{kl}$$

In the above equation, the terms in the first pair of brackets represent the contributions from conventional elastoplasticity theory, and the rest terms represent the contributions from the principal stress rotation. The elastoplastic stiffness tensor E_{ijkl}^{ep} does not depend on the direction of $\dot{\sigma}_{ij}$, indicating an incrementally linear stress-strain relation in the proposed model.

3. Simulation results

The proposed model requires eight material parameters, namely five traditional parameters λ, κ, ν, M_c and M_e, one non-associative flow rule parameter N_c, and two principal stress rotation parameters h_r and d_r. In general, the traditional and flow rule parameters should be calibrated against data from triaxial tests, where the other two parameters h_r and d_r are not operational. Table-1 presents the parameters used in this paper. The traditional parameters are from Banerjee and Yousif [22] for Kaolin and from Whittle [23] for Boston blue clay. The non-associative flow rule parameters are from Jiang *et al.* [15] for both clays.

A validation of the non-associative flow rule using the undrained triaxial compression data of isotopically normally consolidated Kaolin (data from Fannin [24]) is firstly made in Fig 3. The conclusion is consistent with Jiang *et al.* [15], in that the non-associative model can better capture the shear strength of clay than the associative model.

Table 1.
Model parameters for Kaolin and Boston blue clay.

Parameters		Kaolin	Boston blue clay
	λ	0.14	0.184
	κ	0.05	0.034
Traditional	ν	0.3	0.227
	M_c	1.05	1.39
	M_e	0.78	1.12
Non-associative	N_c	0.7	0.95
Principal stress rotation	h_r (kPa)	20000	25000
	d_r	6	7

In Fig 4, the undrained (constant volume) simple shear test on normally consolidated Kaolin is simulated, and the comparisons with the test data from Airey [25] are made. The static lateral stress coefficient K_0 is 0.685 [25]. Three sets of simulation results are presented, respectively made by the associative (i.e. MCC) and non-associative clay models (without the principal stress rotation mechanism), and by the non-associative model incorporating the additional mechanism. It is seen that the associative model significantly overpredicts the undrained shear strength. The non-associative model gives better predictions, and the further inclusion of the principal stress rotation mechanism provides the best match in both the stress-strain response and the stress path. It is therefore evidenced that it is necessary to account for the principal stress rotation if a reasonable prediction is to be achieved for the simple shear. In a previous study by Yang and Yu [11] using a yield-vertex based non-coaxial model, the principal stress rotation affects only the stiffness and not the ultimate shear stress of the soil. The basic difference of their model from the present one is the omission of the plastic volumetric strain in the principal stress rotation mechanism. In the present model, a nonzero D^r enables the principal stress rotation to weaken the conventional plastic loading through the presence of L^r in L^c (see Eqn (14)). Consequently, the yield surface expansion is retarded, and the ultimate stress state, which must lie at the top of the ellipse in the *p-q* plane, is lower. On the other hand, if d_r is chosen to be 0 and therefore $D^r = 0$, the stress-strain response will be similar to that in [11].

Another series of comparisons between the measured and predicted results are presented in Fig 5 for the normally consolidated Boston blue clay. The experimental data from Malek [26] is from a series of undrained simple shear tests under various vertical consolidation stresses ranging between 300-600 kPa. The K_0 for this soil is 0.533 according to [27]. In the simulation, the calculation of excess pore pressure follows the method proposed by Dyvik *et al.* [28] and is estimated as the changes in vertical stress required to keep constant volume throughout a simple shear test. Again, Fig 5 shows that the undrained shear strength is best captured by the non-associative model considering the principal stress rotation, whilst the initial stiffness is somewhat underpredicted by all the simulations, likely due to the ignorance of material anisotropy in the models. The pore pressure predictions are acceptable for all three sets of simulations. As a final investigation, the non-coaxial behaviour of Boston blue clay is shown in Fig 6 using results predicted by the non-associative model incorporating the stress rotation mechanism. The authors are not aware of any detailed experimental analysis on clays' non-coaxiality during simple shearing. Such data on sands obtained from experiments and DEM simulations (e.g. [2,29,30]) showed that during drained simple shear, whilst the major principal stress direction gradually rotates from 0° towards 45°, the major principal plastic (or total) strain rate direction starts from somewhat below 45° and quickly approaches that of the principal stress as the shear strain develops. Results presented in Fig 6 are in very good qualitative agreement with these observations.

4. Conclusions

This paper presents a simple constitutive model dedicated to simulating the clay simple shear behaviour by considering the rarely included factor: the principal stress rotation. The model uses a non-associative flow rule and incorporates an additional mechanism associated with the principal stress rotation. The new mechanism caters for the soil non-coaxiality and plastic volumetric response under pure rotation of principal stress axes. Stress-strain incremental linearity is maintained in the proposed model. The importance of accounting for the principal stress rotation has been justified by comparing the simulations of the proposed model with those from the base models without considering principal stress rotation, and with the clay simple shear experimental data. Whilst the associative model significantly overpredicts the undrained shear strength, the non-associative model can provide better results, and the further inclusion of the principal stress rotation mechanism captures the undrained shear strength with satisfactory. The soil non-coaxial behaviour is also well reproduced.

References

[1] D. Airey, D. Wood, An evaluation of direct simple shear tests on clay. Géotechnique 37 (1) (1987) 25-35.

[2] K. Roscoe, The influence of strains in soil mechanics, Geotechnique 20 (2) (1970) 129-170.

[3] M. Budhu, A. Britto. Numerical analysis of soils in simple shear devices, Soils and Foundations 27 (2) (1987) 31-41.

[4] D Potts, G Dounias, P Vaughan Finite element analysis of the direct shear box test. Geotechnique 37 (1) (1987) 11-23.

[5] G. Dounias, D. Potts, Numerical analysis of drained direct and simple shear tests, Journal of Geotechnical Engineering 119 (12) (1993) 1870-1891.

[6] M. Gutierrez, K. Ishihara, I. Towhata, Model for the deformation of sand during rotation of principal stress directions, Soils and Foundations 33 (3) (1993) 105-117.

[7] Y. Cai, H-S. Yu, D. Wanatowski, X. Li, Noncoaxial behavior of sand under various stress paths, Journal of Geotechnical and Geoenvironmental Engineering 139 (8) (2013) 1381-1395.

[8] S. Nishimura, N. Minh, R. Jardine, Shear strength anisotropy of natural London Clay, Géotechnique 57 (1) (2007) 49-62.

[9] J-G. Qian, Z-B. Du, Z-Y. Yin, Cyclic degradation and non-coaxiality of soft clay subjected to pure rotation of principal stress directions, Acta Geotechnica (2017) 1-17. doi:10.1007/s11440-017-0567-8.

[10] V.A. Osinov, W. Wu, Simple shear in sand with an anisotropic hypoplastic model, Geomechanics and Geoengineering 1 (1) (2006) 43-50. doi:10.1080/17486020600552355.

[11] Y. Yang, H-S. Yu, Numerical simulations of simple shear with non-coaxial soil models, International journal for numerical and analytical methods in geomechanics 30 (1) (2006) 1-19.

[12] M. Gutierrez, J. Wang, M. Yoshimine, Modeling of the simple shear deformation of sand: effects of principal stress rotation, Acta Geotechnica 4 (3) (2009) 193-201.

[13] M. Jefferies, D. Shuttle, K. Been, Principal stress rotation as cause of cyclic mobility, Geotechnical Research 2 (2) (2015) 66-96.

[14] K.H. Roscoe, J.B. Burland, On the generalized stress-strain behaviour of wet clay, In: Heyman J, Leckie FA (eds) Engineering Plasticity, Cambridge, 1968, pp.535-609.

[15] J. Jiang, H.I. Ling, V.N. Kaliakin, An associative and non-associative anisotropic bounding surface model for clay, Journal of Applied Mechanics 79 (3) (2012) 031010.

[16] D. Sheng, S.W. Sloan, H-S. Yu, Aspects of finite element implementation of critical state models, Computational mechanics 26 (2) (2000) 185-196.

[17] Z. Gao, J. Zhao, A non-coaxial critical-state model for sand accounting for fabric anisotropy and fabric evolution, International Journal of Solids and Structures 106 (2017) 200-212.

[18] K. Hashiguchi, Elastoplasticity theory, Springer, Berlin, 2014.

[19] N. Lu, Y. Yang, H-S. Yu, Comparison of yield-vertex tangential loading and principal stress rotational loading, Computers and Geotechnics, 108 (2019) 88-94. doi: 10.1016/j.compgeo.2018.12.009

[20] K. Miura, S. Miura, S. Toki, Deformation behavior of anisotropic dense sand under principal stress axes rotation, Soils and Foundations 26 (1) (1986) 36-52.

[21] Z. Yang, X. Li, J. Yang, Undrained anisotropy and rotational shear in granular soil, Geotechnique (2007)

[22] P. Banerjee, N. Yousif, A plasticity model for the mechanical behaviour of anisotropically consolidated clay, International Journal for Numerical and Analytical Methods in Geomechanics 10 (5) (1986) 521-541.

[23] A. Whittle, Evaluation of a constitutive model for overconsolidated clays, Geotechnique 43 (2) (1993) 289-313.

[24] R.J. Fannin, Geogrid reinforcement of granular layers on soft clay-a study at model and full scale, PhD thesis, University of Oxford, UK, 1986.

[25] D.W. Airey, Clays in circular simple shear apparatus, University of Cambridge, UK, 1984.

[26] A.M. Malek, Cyclic behavior of clay in undrained simple shearing and application to offshore tension piles, Massachusetts Institute of Technology, USA, 1987.

[27] A.G. Papadimitriou, M.T. Manzari, Y.F. Dafalias, Calibration of a simple anisotropic plasticity model for soft clays, In: Geo-Frontiers Congress, Austin, Texas, United States, (2005) pp.415-424. doi:10.1061/40771(169)18

[28] R. Dyvik, T. Berre, S. Lacasse, B. Raadim, Comparison of truly undrained and constant volume direct simple shear tests, Geotechnique 37(1) (1987), 3-10.

[29] C. Thornton, L. Zhang, A numerical examination of shear banding and simple shear non-coaxial flow rules, Philosophical Magazine 86 (21-22) (2006) 3425-3452. doi:10.1080/14786430500197868

[30] J. Ai, P.A. Langston, H-S. Yu, Discrete element modelling of material non-coaxiality in simple shear flows, International Journal for Numerical and Analytical Methods in Geomechanics 38 (6) (2014) 615-635.

TABLES

Table-1. Model parameters for Kaolin and Boston blue clay

Parameters		Kaolin	Boston blue clay
Traditional	λ	0.14	0.184
	κ	0.05	0.034
	v	0.3	0.227
	M_c	1.05	1.39
	M_e	0.78	1.12
Non-associative	N_c	0.7	0.95
Principal stress rotation	h_r (kPa)	20000	25000
	d_r	6	7
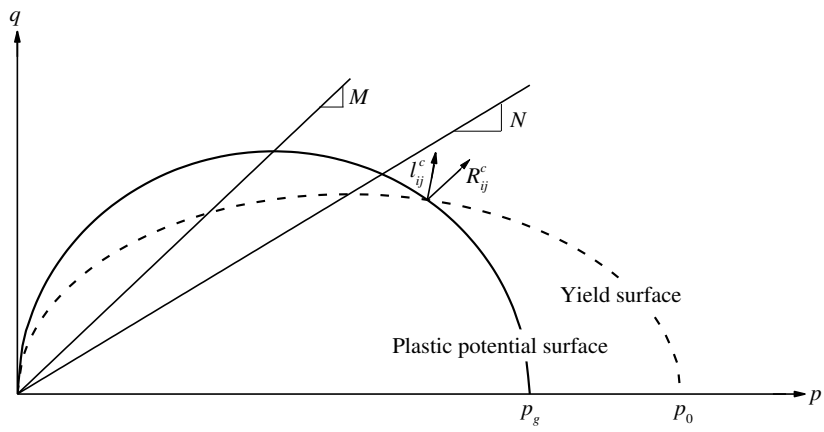
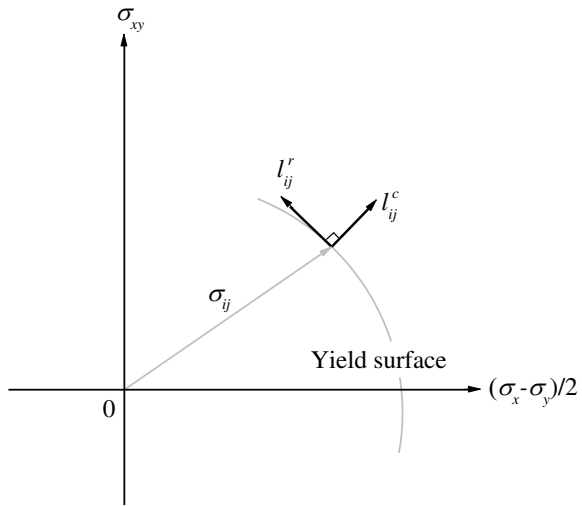Fig 1. Schematic illustration of the non-associative clay plasticity model in the *p-q* plane.

Fig 2. Schematic illustration of the definition of the loading direction l_{ij}^r in the plane of $((\sigma_x - \sigma_y)/2, \sigma_{xy})$.
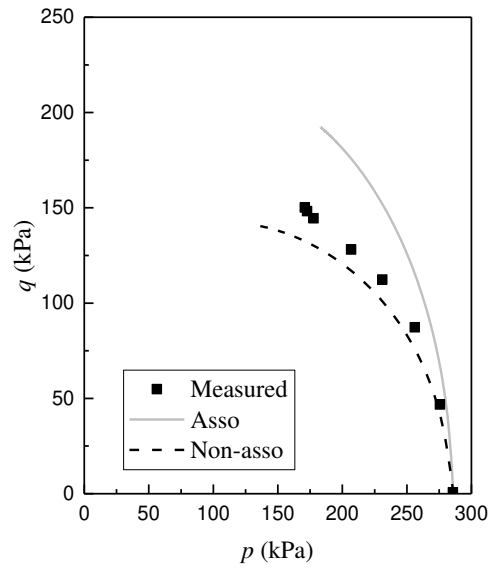
Fig 3. Validation of the non-associative flow rule against undrained triaxial compression test data of isotopically normally consolidated Kaolin (experimental data from [24]).
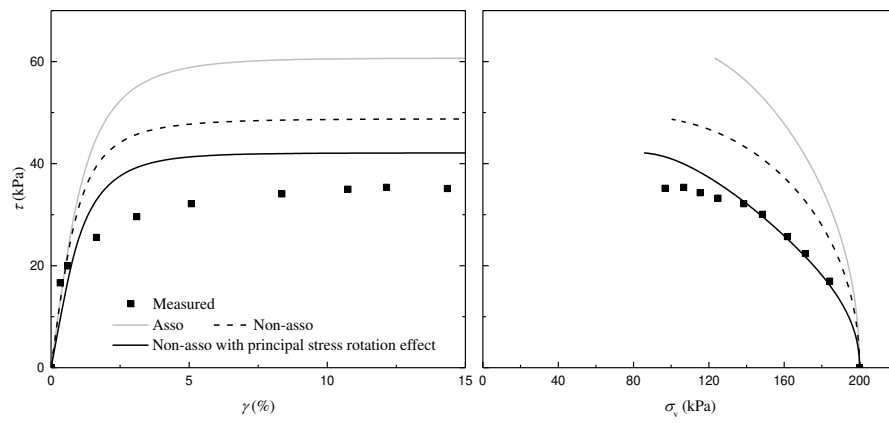
Fig 4. Comparison of measured and predicted stress-strain response and stress path for undrained simple shear on normally consolidated Kaolin (experimental data from [25]).
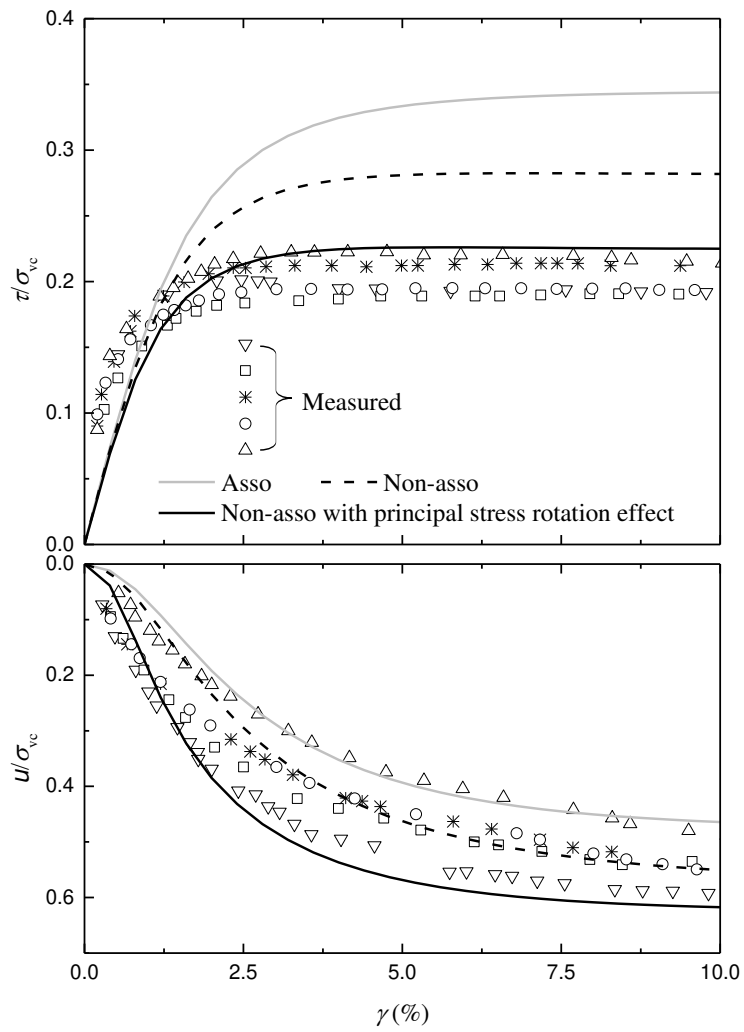
Fig 5. Comparison of measured and predicted normalized stress-strain and excess pore pressure responses for undrained simple shear on normally consolidated Boston blue clay (experimental data from [26]).
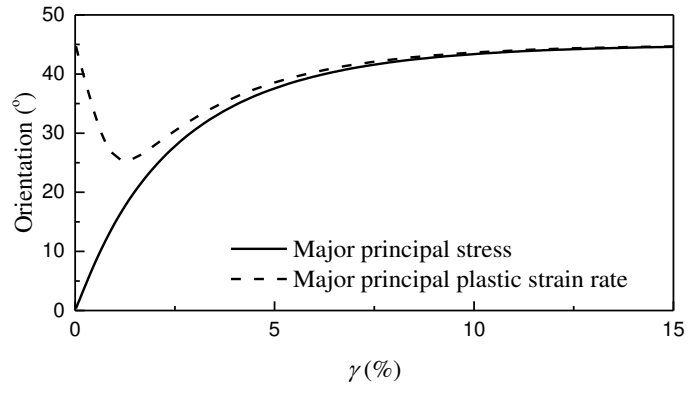
Fig 6. Predicted non-coaxiality evolution for undrained simple shear on Boston blue clay.